Physics Letters B 697 (2011) 471–476

Contents lists available at ScienceDirect

Physics Letters B

www.elsevier.com/locate/physletb

Symmetry energy from elliptic flow in $^{197}Au + ^{197}Au$

P. Russotto [a], P.Z. Wu [b], M. Zoric [c,d], M. Chartier [b], Y. Leifels [c], R.C. Lemmon [e], Q. Li [f], J. Łukasik [c,g], A. Pagano [h], P. Pawłowski [g], W. Trautmann [c,*]

[a] INFN-LNS and Università di Catania, I-95123 Catania, Italy
[b] University of Liverpool, Physics Department, Liverpool L69 7ZE, United Kingdom
[c] GSI Helmholtzzentrum für Schwerionenforschung GmbH, D-64291 Darmstadt, Germany
[d] Ruder Bošković Institute. HR-10002 Zagreb, Croatia
[e] STFC Daresbury Laboratory, Warrington WA4 4AD, United Kingdom
[f] School of Science, Huzhou Teachers College, Huzhou 313000, China
[g] IFJ-PAN, Pl-31342 Kraków, Poland
[h] INFN-Sezione di Catania, I-95123 Catania, Italy

ARTICLE INFO

Article history:
Received 19 October 2010
Received in revised form 12 January 2011
Accepted 11 February 2011
Available online 16 February 2011
Editor: V. Metag

Keywords:
Heavy ion collisions
Elliptic flow
Symmetry energy

ABSTRACT

The elliptic-flow ratio of neutrons with respect to protons or light complex particles in reactions of neutron-rich systems at relativistic energies is proposed as an observable sensitive to the strength of the symmetry term in the equation of state at supra-normal densities. The results obtained from the existing FOPI/LAND data for $^{197}Au + ^{197}Au$ collisions at 400 MeV/nucleon in comparison with the UrQMD model favor a moderately soft symmetry term with a density dependence of the potential term proportional to $(\rho/\rho_0)^\gamma$ with $\gamma = 0.9 \pm 0.4$.

Recent advances in the observation and modelling of astrophysical phenomena have renewed the interest in the nuclear equation of state (EOS) and, in particular, in its dependence on density and on asymmetry, i.e., on the relative neutron-to-proton abundance [1–3]. Supernova simulations or neutron star models require inputs for the nuclear EOS at extreme values of these parameters [4,5]. The dependence on asymmetry is given by the symmetry term whose evolution with density is not only of interest for astrophysics but also for nuclear physics. The thickness of the neutron skin of heavy nuclei, e.g., reflects the differential pressure exerted on neutrons in the core [6], and the strength of the three-body force, an important ingredient in nuclear structure calculations [7], represents one of the major uncertainties in modelling the EOS at high density [1,8].

Considerable efforts are, therefore, underway in using heavy-ion reactions for extracting experimental information on the symmetry energy which is the difference between the energy of neutron matter and of symmetric matter. While fairly consistent constraints for the symmetry energy near normal nuclear matter density have been deduced from recent data [3,9–11], much more work is still needed to probe its high-density behavior. The predictions of microscopic models diverge widely there [3,12], and the interpretation of obvious observables turns out to be more difficult than perhaps anticipated. The ratios of K^+/K^0 production were found to be less sensitive to the symmetry energy when actual collisions were modelled rather than matter under equilibrium conditions [13]. Variations of the π^-/π^+ ratio of up to 20% for soft versus stiff parameterizations are expected but the competition of mean-field and collision effects appears to be very delicate. Different predictions leading to practically opposite conclusions were obtained from the comparison of the FOPI data for $^{197}Au + ^{197}Au$ collisions [14] with different transport models [15–17].

It seems essential, in this situation, to enlarge the experimental basis of suitable probes and to extend it from isotopic yield ratios to the isospin dependence of dynamical observables. Densities of up to 2 or 3 times the saturation density may be reached within a short time scale (≈ 20 fm/c) in the central zone of heavy-ion collisions in the present range of relativistic energies of up to ≈ 1 GeV/nucleon [18]. The resulting pressure produces a collective outward motion of the compressed material whose strength will be influenced by the symmetry energy in asymmetric systems [19]. Flow observables have been proposed by several groups as probes for the equation of state at high density [20,21], among them the so-called differential neutron–proton flow which is the difference

* Corresponding author.
E-mail address: w.trautmann@gsi.de (W. Trautmann).

0370-2693
doi:10.1016/j.physletb.2011.02.033

of the parameters describing the collective motion of free neutrons and protons weighted by their numbers [20]. As pointed out by Yong et al. [22], this observable minimizes the influence of the isoscalar part in the EOS while maximizing that of the symmetry term. Its proportionality to the particle multiplicities, however, makes its determination very dependent on the experimental efficiencies of particle detection and identification and on the precise theoretical distinction between free and bound nucleons. In this work, the ratios of neutron versus proton or light-charged-particle flows will be considered and their sensitivities to the strength of the symmetry term will be explored. The problem of systematic errors is thereby reduced.

In a series of experiments at the GSI laboratory combining the LAND and FOPI (Phase 1) detectors, both neutron and hydrogen collective flow observables from ^{197}Au + ^{197}Au collisions at 400, 600 and 800 MeV/nucleon have been measured [23,24]. These data sets are presently being reanalyzed in order to determine optimum conditions for a dedicated new experiment, but also with the aim to produce constraints for the symmetry energy by comparing with predictions of state-of-the-art transport models. Here, we report the results obtained with the 400-MeV/nucleon data set and the Ultrarelativistic-Quantum-Molecular-Dynamics (UrQMD) model which has recently been adapted to heavy ion reactions at intermediate energies [25].

The Large-Area-Neutron-Detector LAND is a $2 \times 2 \times 1$ m^3 calorimeter consisting of in total 200 slabs of interleaved iron and plastic strips viewed by photomultiplier tubes at both ends [26]. For the flow experiment, LAND was divided into two parts of 50-cm depth each, positioned to cover laboratory angles of 37°–53° and 61°–85°. The corresponding acceptance in the plane of transverse momentum p_t vs. rapidity y is shown in Fig. 1. Veto walls of 5-mm-thick plastic scintillators in front of the two detector units permitted the distinction of neutral and charged particles and to resolve atomic numbers $Z \leqslant 2$. A shower-recognition algorithm is used to identify individual particles within the registered hit distributions. Particle momenta were determined from the measured time-of-flight ($\Delta t \approx 550$ ps, FWHM) over flight paths of 5 m and 7 m to the more backward and more forward detector units, respectively. The amount of light collected from identified showers was used to generate mass spectra of the hydrogen isotopes as described in Ref. [24]. Individual isotopic resolution is not achieved but the strong proton group is clearly identified. The selected proton samples, containing about 45% of the total hydrogen yields, are expected to have isotopic purity of better than 95%.

During its Phase 1, the 4-π detector FOPI consisted of a forward plastic array, built from more than 700 individual plastic-scintillator strips and covering the forward hemisphere at laboratory angles from 1° to 30° [27]. LAND was used to detect and identify neutrons and light charged particles with nearly identical methods while the FOPI Forward Wall was used to determine the modulus and orientation of the impact parameter from the multiplicity M_c and azimuthal distribution of the detected charged particles [28]. In the analysis, events were grouped into 5 event classes labelled PM1 (most peripheral) to PM5 (most central) according to the recorded multiplicity M_c. The background of scattered neutrons was measured in separate runs with shadow bars made from iron and positioned to block the direct flight paths from the target to one or the other of the two LAND units. Additional details can be found in Refs. [23,24].

The usefulness of the studied observables has been evaluated with the UrQMD transport model [25]. This model, originally developed to study particle production at high energy [29], has been adapted to intermediate-energy heavy-ion collisions by introducing a nuclear mean field corresponding to a soft EOS with momentum dependent forces and with different options for the dependence

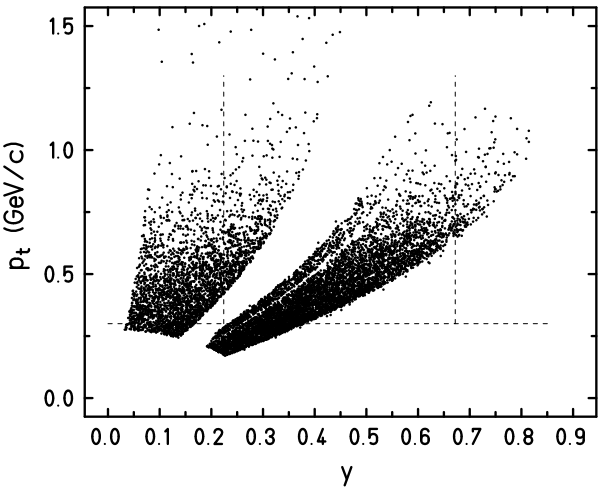

Fig. 1. Scatter plot of 10000 neutron events with energy $E_{\rm lab} \geqslant 40$ MeV from a run without shadow bars in the plane of transverse momentum p_t vs. rapidity y. The quality criteria are the same as used in the flow analysis. Their application produces the local inefficiency in the forward detector unit caused by slabs with reduced performance. The dashed lines represent the acceptance cuts $p_t \geqslant 0.3$ GeV/c and $0.25 \leqslant y/y_p \leqslant 0.75$ applied later in the analysis.

on asymmetry. Two of these choices are used here, expressed as a power-law dependence of the potential part of the symmetry energy on the nuclear density ρ according to

$$E_{\rm sym} = E_{\rm sym}^{\rm pot} + E_{\rm sym}^{\rm kin} = 22\ {\rm MeV} \cdot (\rho/\rho_0)^{\gamma} + 12\ {\rm MeV} \cdot (\rho/\rho_0)^{2/3} \quad (1)$$

with $\gamma = 0.5$ and $\gamma = 1.5$ corresponding to a soft and a stiff density dependence (ρ_0 is the normal nuclear density of ≈ 0.16 fm^{-3}). The kinetic part remains unchanged. The UrQMD model has been successfully used for studies of a wide range of heavy-ion-collision problems at intermediate and relativistic energies (Ref. [30] and references given therein).

As mentioned above, a realistic description of the clustering processes during the temporal evolution of the reaction is crucial for predicting dynamical properties of free neutrons, protons and light charged particles. In the UrQMD, the clustering algorithm is based on the proximity of nucleons in phase space with two parameters for the relative nucleon coordinates and momenta. The present analysis was performed with the distributions obtained after a reaction time of 150 fm/c and with the proximity limits $\Delta r = 3.0$ fm and $\Delta p = 275$ MeV/c which are typical for QMD models [31]. These parameters had been slightly adjusted from their default values in order to obtain a best possible description of measured fragment spectra as a function of Z. The result for central collisions of ^{197}Au + ^{197}Au at 400 MeV/nucleon is shown in Fig. 2 in comparison with the data of Reisdorf et al. [28]. With a normalization at $Z = 1$, the overall dependence on Z is rather well reproduced but the yields of $Z = 2$ particles are underpredicted by about a factor of 3. The strong binding of α particles is beyond the phase-space criterion used in the model. However, also the 4-π integrated yields of deuterons and tritons in central collisions are underestimated by similar factors of 2–3.

Flow observables were obtained from the calculated event samples by fitting the azimuthal particle distributions with the usual Fourier expansion

$$f(\Delta\phi) \propto 1 + 2 \cdot v_1 \cdot \cos(\Delta\phi) + 2 \cdot v_2 \cdot \cos(2 \cdot \Delta\phi) \quad (2)$$

with $\Delta\phi$ representing the azimuthal angle of the momentum vector of the emitted particle with respect to the reaction plane [32]. The predictions obtained for the elliptic flow of neutrons, protons,

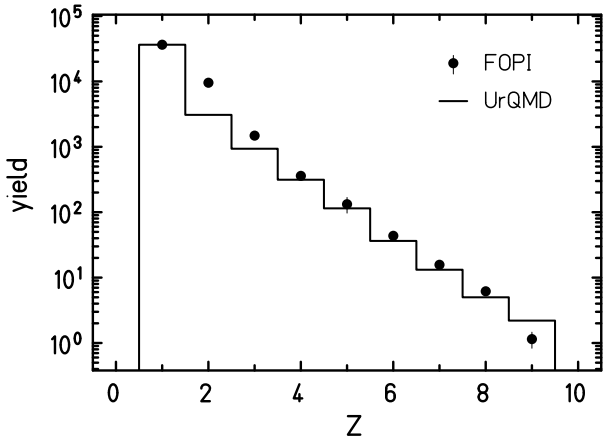

Fig. 2. Fragment yields, integrated over the 4-π solid angle, in central (equivalent to $b < 2.0$ fm) collisions of ^{197}Au + ^{197}Au at 400 MeV/nucleon as a function of Z (dots, from Ref. [28]) in comparison with UrQMD predictions normalized at $Z = 1$ (histogram).

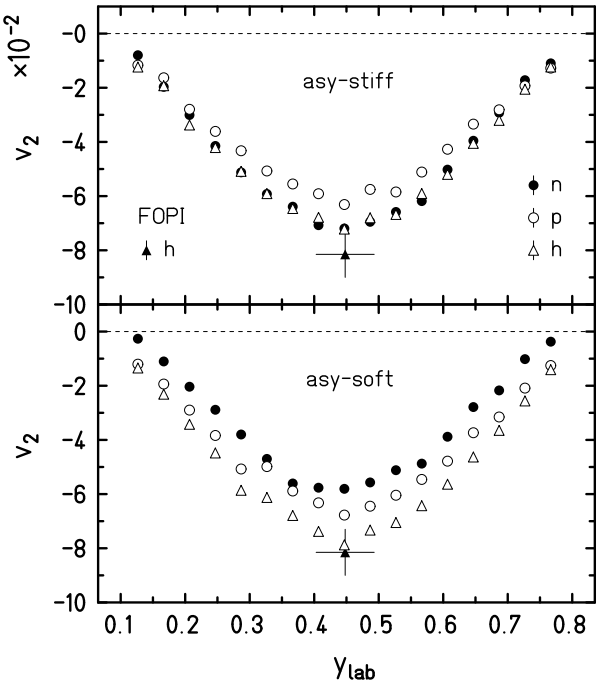

Fig. 3. Elliptic flow parameter v_2 for mid-peripheral ($5.5 \leqslant b \leqslant 7.5$ fm) ^{197}Au + ^{197}Au collisions at 400 MeV/nucleon as calculated with the UrQMD model for neutrons (dots), protons (circles), and all hydrogen isotopes ($Z = 1$, open triangles), integrated over transverse momentum p_t, as a function of the laboratory rapidity $y_{\rm lab}$. The predictions obtained with a stiff and a soft density dependence of the symmetry term are given in the upper and lower panels, respectively. The experimental result from Ref. [33] for $Z = 1$ particles at mid-rapidity is represented by the filled triangle (the horizontal bar represents the experimental rapidity interval).

and hydrogen yields for ^{197}Au + ^{197}Au at 400 MeV/nucleon and for the two choices of the density dependence of the symmetry energy, labeled asy-stiff ($\gamma = 1.5$) and asy-soft ($\gamma = 0.5$), are shown in Fig. 3. The dominant difference is the significantly larger neutron squeeze-out in the asy-stiff case (upper panel) compared to the asy-soft case (lower panel). The proton and hydrogen flows respond only weakly, and in opposite direction, to the variation of γ within the chosen interval.

Collective flow has recently been measured rather systematically [33]. The reliability of the methods has been demonstrated by the good agreement of data sets from different experiments in the overlap regions of the studied intervals in collision energy [32]. An excitation function of flow for ^{197}Au + ^{197}Au collisions has been produced for incident energies from below 100 MeV/nucleon up to the ultrarelativistic regime. Within this wide range, the negative elliptic flow of light particles, i.e. their squeeze-out perpendicular to the reaction plane, has its maximum at 400 MeV/nucleon. The value $v_2 = -0.082$ measured at this energy for $Z = 1$ particles at mid-rapidity [33] is reasonably well reproduced by the UrQMD model, even though underestimated by 8% and 15% with the two parameterizations (Fig. 3).

The predictions for elliptic particle flows depend strongly on the type of transport theory used and on its parameters. Values lower than found experimentally have been reported also for other models as, e.g., discussed in Refs. [31,34]. In a recent paper, Li et al. investigate the elastic in-medium nucleon–nucleon cross section and show the effects of its momentum dependence on various observables [35]. The standard parameterization, also used here up to now, is labeled FP1 in that paper. One of the alternatives, FP2, exhibits a higher correction factor than FP1 for relative nucleon–nucleon momenta around $0.2 < p_{\rm NN} < 0.5$ GeV/c at high density. With this parameterization, the elliptic flow is larger, now exceeding the measured $Z = 1$ value by 16% and 19% for the stiff and soft parameterizations of the symmetry term, respectively.

The results obtained from the FOPI/LAND data set for 400 MeV/nucleon are shown in Fig. 4 as a function of the rapidity y, normalized with respect to the projectile rapidity $y_p = 0.896$, and for the PM3 event class ($27 \leqslant M_c \leqslant 39$) which approximately corresponds to the interval of impact parameters 5.5 fm $\leqslant b \leqslant$ 7.5 fm [28]. The geometrical acceptance of the LAND detector in this experiment produces a dependence of the accepted range in transverse momentum p_t on rapidity y, p_t increases with y (Fig. 1), and is responsible for the observed asymmetry of v_1 and v_2 with respect to mid-rapidity $y/y_p = 0.5$. Gates were set for transverse momenta $0.3 \leqslant p_t/A \leqslant 1.3$ GeV/c, mainly to ensure equal lower thresholds for neutrons and charged particles detected with LAND. For the comparison, the UrQMD outputs have been filtered with the geometrical acceptance of the LAND detector and subjected to the same transverse-momentum gates as the experimental data. The experimental Fourier coefficients, on the other hand, have been corrected for the uncertainty associated with the reconstruction of the reaction plane from the azimuthal distribution of particles measured with the FOPI Forward-Wall detector. Because of the significant multiplicities $M_c > 26$ of particles observed in the considered range of impact parameters $b \leqslant 7.5$ fm, this correction is not crucial [32], and global correction factors 1.05 for v_1 and 1.15 for v_2 have been adopted.

Only the predictions for neutrons, obtained with the standard FP1 parameterization of the elastic nucleon–nucleon cross section [35], are shown in Fig. 4, for clarity as well as because of the much smaller dependence on γ of the results for hydrogen isotopes (cf. Fig. 3). A nearly negligible sensitivity to the stiffness of the symmetry energy is exhibited by the directed flow, according to the UrQMD model (Fig. 4, top panel). The lines representing the predictions for the soft and stiff parameterizations of the symmetry energy fall practically on top of each other. The results for protons or hydrogen isotopes are nearly identical. All predictions compare well, however, with the experimental results for the multiplicity bin PM3 corresponding to this range of mid-peripheral impact parameters. The range of rapidities $y \geqslant 0.8$ at which the data deviate from the expected linearity coincides with the shift of the LAND acceptance to transverse momenta $p_t \geqslant 0.75$ GeV/c/nucleon at which the yields start to drop rapidly (Fig. 1).

Also the second Fourier coefficient v_2 describing elliptic flow and its dependence on rapidity is fairly well reproduced by the UrQMD calculations (Fig. 4, bottom panel). Here the statistical er-

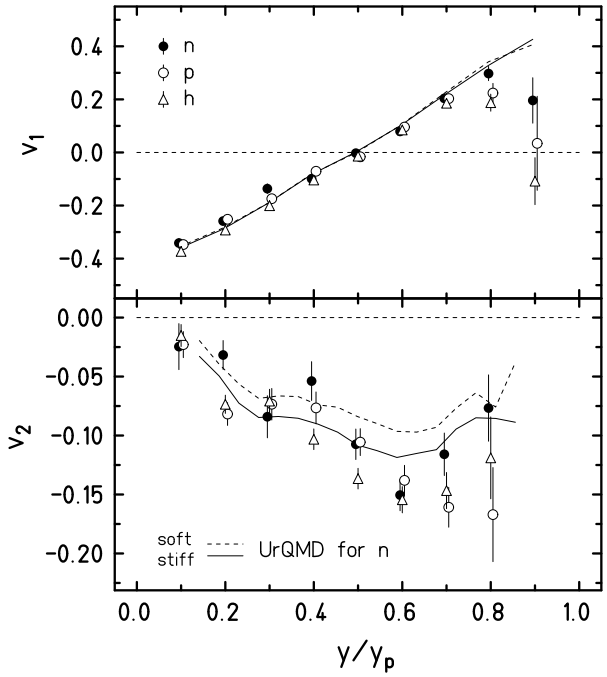

Fig. 4. Measured flow parameters v_1 (top) and v_2 (bottom) for mid-peripheral ($5.5 \leqslant b \leqslant 7.5$ fm) ^{197}Au + ^{197}Au collisions at 400 MeV/nucleon for neutrons (dots), protons (circles), and hydrogen isotopes ($Z = 1$, open triangles) integrated within $0.3 \leqslant p_t/A \leqslant 1.3$ GeV/c/nucleon as a function of the normalized rapidity $y_{\rm lab}/y_p$. The UrQMD predictions for neutrons, obtained with a stiff ($\gamma = 1.5$, full lines) and a soft ($\gamma = 0.5$, dashed) density dependence of the symmetry term have been filtered to correspond to the geometrical acceptance of the experiment. The experimental data have been corrected for the dispersion of the reaction plane (see text).

rors of the experimental data are larger but the slight underprediction expected from Fig. 3 is clearly recognized. Contrary to the directed flow, the v_2 values calculated with the asy-stiff and asy-soft parameterizations for neutrons are significantly different from each other. This is not the case for the hydrogen isotopes whose squeeze-out parameters are close to those of neutrons for the asy-stiff case or, for free protons alone, similar to the asy-soft neutron predictions. Even though the experimental errors are considerable, the sensitivity of the neutron squeeze-out seems large enough to permit the extraction of a useful result from the present data set.

The dependence of the elliptic flow parameter v_2 on the transverse momentum per nucleon, p_t/A, is shown in Fig. 5, upper panel, for the combined data set of central and mid-peripheral collisions (PM3–PM5, $M_c \geqslant 27$, cf. Ref. [28]) in order to exploit the full statistics collected in the experiment. The extreme rapidities are avoided by selecting the interval $0.25 \leqslant y/y_p \leqslant 0.75$. The increase of v_2 in absolute magnitude is nearly linear and the measured values for neutrons and hydrogen isotopes follow approximately the UrQMD predictions for $b < 7.5$ fm. For hydrogens (not shown), the results for the stiff and soft density dependences are similar and close to the asy-stiff predictions for neutrons. For neutrons, however, the predictions are different by, on average, 20% for the main part of the p_t interval (dashed lines) but seem to converge at high p_t at which the yields become small and the statistical errors large.

For the quantitative evaluation, the ratio of the flow parameters of neutrons versus hydrogen isotopes is proposed to be used. Systematic effects influencing the collective flows of neutrons and charged particles in similar ways will be minimized in this way, on the experimental as well as on the theoretical side. Among them are, in particular, the still existing uncertainties of isoscalar type in the EOS but also, e.g., the dispersion of the experimentally determined orientation of the reaction plane, possible small azimuthal

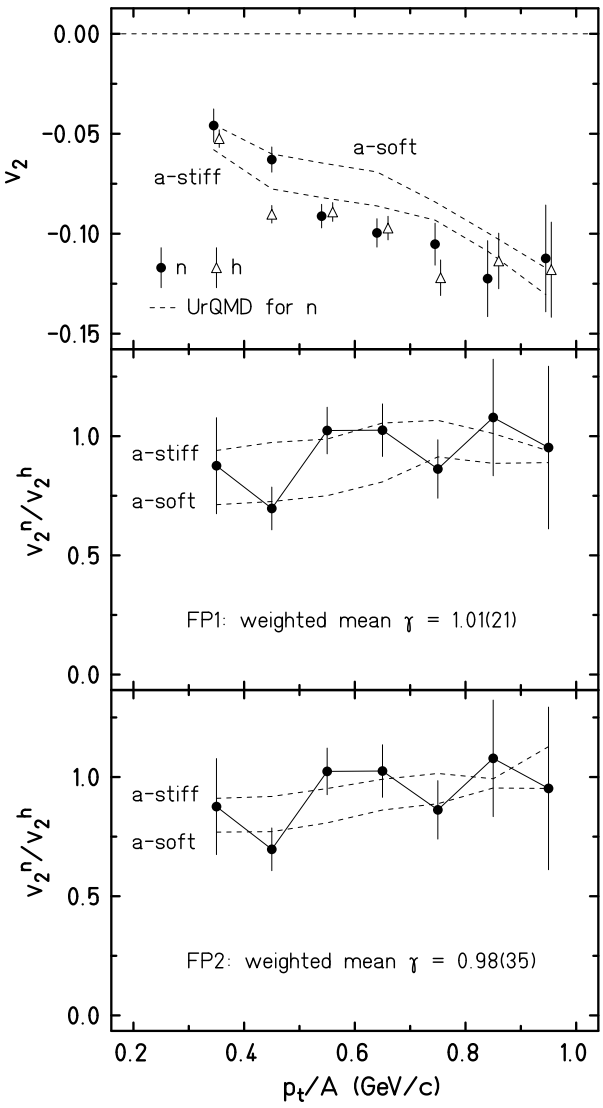

Fig. 5. Elliptic flow parameters v_2 for neutrons (dots) and hydrogen isotopes (open triangles, top panel) and their ratio (lower panels) for moderately central ($b < 7.5$ fm) collisions of ^{197}Au + ^{197}Au at 400 MeV/nucleon, integrated within the rapidity interval $0.25 \leqslant y/y_p \leqslant 0.75$, as a function of the transverse momentum per nucleon p_t/A. The symbols represent the experimental data. The UrQMD predictions for $\gamma = 1.5$ (a-stiff) and $\gamma = 0.5$ (a-soft) obtained with the FP1 parameterization for neutrons (top panel) and for the ratio (middle panel), and with the FP2 parameterization for the ratio (bottom panel) are given by the dashed lines. Note the suppressed zero of the abscissa.

anisotropies in the particle detection with the Forward Wall, and the matching of the impact-parameter intervals used in the calculations with the experimental event groups selected according to multiplicity.

The results for the ratio v_2^n/v_2^h, i.e. with respect to the integrated hydrogen yield, are shown in Fig. 5 (lower panels). They exhibit once more the sensitivity of the elliptic flow to the stiffness of the symmetry energy predicted by the UrQMD. It is slightly smaller with the FP2 parameterization of the in-medium nucleon-nucleon cross section (bottom panel). The experimental ratios, even though associated with large errors, are found to scatter within the intervals given by the calculations for $\gamma = 0.5$ and 1.5 in either case, indicating that the effects of the cross section parameterization largely cancel in the ratios. Linear interpolations between the predictions, averaged over $0.3 < p_t/A \leqslant 1.0$ GeV/c with weights $(\Delta\gamma_i)^{-2}$ derived from the experimental errors $\Delta\gamma_i$

for each p_t bin, yield $\gamma = 1.01 \pm 0.21$ and $\gamma = 0.98 \pm 0.35$ for the FP1 and FP2 parameterizations, respectively.

The same analysis was also performed for the squeeze-out ratios v_2^n/v_2^p of neutrons with respect to free protons. The resulting power-law exponents are $\gamma = 0.99 \pm 0.28$ and $\gamma = 0.85 \pm 0.47$ for the FP1 and FP2 parameterizations, respectively. They are nearly identical to those obtained from the neutron-to-hydrogen squeeze-out ratios, even though associated with larger statistical uncertainties. If the comparisons of the neutron-to-hydrogen ratios v_2^n/v_2^h are restricted to the mid-peripheral interval of impact-parameters $5.5 \leqslant b < 7.5$ fm, smaller values $\gamma = 0.58 \pm 0.27$ and $\gamma = 0.35 \pm 0.44$ are obtained with the FP1 and FP2 parameterizations, respectively. This apparent dependence on impact parameter existed already in preliminary results reported earlier [36].

All results are, within errors, compatible with each other. In particular, the fact that the yields of deuterons and tritons with respect to protons are underestimated in the model calculations does not seem to have visible consequences. The ratios with respect to all hydrogen isotopes and to protons alone yield the same exponent γ. However, because of the limited statistical accuracy, the existence of systematic uncertainties cannot be ruled out and may, in fact, be partly responsible for the apparent dependence on impact parameter. We will, therefore, assume that the difference between the weighted means of the four results for $b < 7.5$ fm and the full statistics, $\gamma = 0.98$, and of the two values for v_2^n/v_2^h and the mid-peripheral range $5.5 \leqslant b < 7.5$ fm, $\gamma = 0.52$, can serve as an estimate, $\Delta\gamma|_{\text{syst.}} = \pm 0.23$, for the magnitude of possible systematic uncertainties.

The statistical errors of the elliptic flow coefficients translate into statistical errors of γ that depend on the sensitivity displayed by the predictions (Fig. 5, lower panels). Since the magnitude of elliptic flow is either slightly underpredicted or overpredicted with the two parameterizations, we interpolate between the two cases and obtain $\Delta\gamma|_{\text{stat.}} = \pm 0.27$ as the most probable statistical error. Combining it with the systematic uncertainty and considering the spread and trends of the individual results, we adopt the value $\gamma = 0.9 \pm 0.4$ as the result of this analysis for the exponent describing the density dependence of the potential term. Together with the kinetic term proportional to $(\rho/\rho_0)^{2/3}$, the squeeze-out data thus indicate a moderately soft behavior of the symmetry energy. It is obvious that data with higher statistical precision are highly desirable. Being able to follow the evolutions with impact parameter, transverse momentum (cf. Fig. 5) and particle type more accurately will provide supplementary constraints for the comparison with theory and will permit a clearer identification of systematic dependences related to it.

Other systematic errors were found to be comparatively minor. In the experimental data analysis, the explored variations of the conditions and gates within reasonable limits have only small effects. The uncertainty associated with the procedures used to measure and subtract the background of scattered neutrons detected with LAND [23,24] has been estimated by subtracting only 60% instead of 100% of the measured background contributions from the total neutron yields. It reduces the resulting power-law exponent γ by $|\Delta\gamma| \approx 0.2$ which may be considered an upper limit for systematic experimental effects.

Additional systematic uncertainties on the theoretical side have also been evaluated. In particular, a test has been made whether supra-saturation densities are actually probed by the squeeze-out ratios. The coefficient of the potential term in the symmetry energy has been reduced from its default value 22 MeV to 18 MeV (cf. Eq. (1)). A softer (stiffer) density dependence is expected in this case if the symmetry term were mainly tested at densities below (above) saturation. The result obtained for v_2^n/v_2^h with FP1, $\gamma = 0.93 \pm 0.28$, is close to the corresponding $\gamma = 1.01 \pm 0.21$ obtained with 22 MeV, thus confirming that the dynamics at supra-saturation density are important for the comparison. The parameter L, proportional to the slope of the symmetry term at saturation [3] changes by less than 20 MeV when this modification is made. The adopted result $\gamma = 0.9 \pm 0.4$ corresponds to $L = 83 \pm 26$ MeV in the standard parameterization with 22 MeV.

In summary, the ratio of the elliptic-flow parameters of neutrons with respect to hydrogen isotopes measured for ^{197}Au + ^{197}Au collisions at 400 MeV/nucleon in the FOPI/LAND experiment has been used to determine the strength of the symmetry term in the equation of state by comparing it to UrQMD model predictions. A value of $\gamma = 0.9 \pm 0.4$ has been obtained for the power-law coefficient describing the density dependence of the potential term. Individual systematic errors were not found to exceed a margin of $|\Delta\gamma| \approx 0.2$. Together with the kinetic term proportional to $(\rho/\rho_0)^{2/3}$, this indicates a moderately soft symmetry term. Within errors, it is consistent with the density dependence deduced from fragmentation experiments probing nuclear matter near or below saturation [9–11] but inconsistent with the super-soft or extremely stiff behavior obtained from the comparisons of the π^-/π^+ yield ratios measured for the same reaction with different transport models [16,17]. Further experimental and theoretical work will be needed to resolve these apparent ambiguities.

Acknowledgements

Illuminating discussions with Lie-Wen Chen, M. Di Toro, Bao-An Li, W. Reisdorf, and H.H. Wolter are gratefully acknowledged. This work has been supported by the European Community under contract No. HPRI-CT-1999-00001 and FP7-227431 (Hadron-Physics2), by the United Kingdom Science and Technology Facilities Council and Engineering and Physical Sciences Research Council, by the Ministry of Education of China under grant No. 209053, by the National Natural Science Foundation of China under grant Nos. 10905021 and 10979023, by the Zhejiang Provincial Natural Science Foundation of China under grant No. Y6090210, and by the Polish Ministry of Science and Higher Education under grant No. DPN/N108/GSI/2009.

References

[1] C. Fuchs, H.H. Wolter, Eur. Phys. J. A 30 (2006) 5.
[2] T. Klähn, et al., Phys. Rev. C 74 (2006) 035802.
[3] For a recent review, see Bao-An Li, Lie-Wen Chen, Che Ming Ko, Phys. Rep. 464 (2008) 113.
[4] J.M. Lattimer, M. Prakash, Phys. Rep. 333 (2000) 121.
[5] A.S. Botvina, I.N. Mishustin, Phys. Lett. B 584 (2004) 233; A.S. Botvina, I.N. Mishustin, Nucl. Phys. A 843 (2010) 98.
[6] C.J. Horowitz, J. Piekarewicz, Phys. Rev. Lett. 86 (2001) 5647.
[7] R.B. Wiringa, S.C. Pieper, Phys. Rev. Lett. 89 (2002) 182501.
[8] Chang Xu, Bao-An Li, Phys. Rev. C 81 (2010) 064612.
[9] A. Klimkiewicz, et al., Phys. Rev. C 76 (2007) 051603(R).
[10] M. Centelles, X. Roca-Maza, X. Viñas, M. Warda, Phys. Rev. Lett. 102 (2009) 122502.
[11] M.B. Tsang, et al., Phys. Rev. Lett. 102 (2009) 122701.
[12] Ph. Chomaz, F. Gulminelli, W. Trautmann, S.J. Yennello (Eds.), Dynamics and Thermodynamics with Nuclear Degrees of Freedom, Eur. Phys. J. A 30 (2006), Springer, Berlin/Heidelberg/New York.
[13] X. Lopez, et al., Phys. Rev. C 75 (2007) 011901(R).
[14] W. Reisdorf, et al., Nucl. Phys. A 781 (2007) 459.
[15] G. Ferini, et al., Phys. Rev. Lett. 97 (2006) 202301.
[16] Zhigang Xiao, et al., Phys. Rev. Lett. 102 (2009) 062502.
[17] Zhao-Qing Feng, Gen-Ming Jin, Phys. Lett. B 683 (2010) 140.
[18] Bao-An Li, Nucl. Phys. A 708 (2002) 365.
[19] P. Danielewicz, R. Lacey, W.G. Lynch, Science 298 (2002) 1592.
[20] Bao-An Li, Phys. Rev. Lett. 88 (2002) 192701.
[21] V. Greco, et al., Phys. Lett. B 562 (2003) 215.
[22] Gao-Chan Yong, Bao-An Li, Lie-Wen Chen, Phys. Rev. C 74 (2006) 064617.
[23] Y. Leifels, et al., Phys. Rev. Lett. 71 (1993) 963.

[24] D. Lambrecht, et al., Z. Phys. A 350 (1994) 115.
[25] Q. Li, et al., J. Phys. G 31 (2005) 1359;
Q. Li, et al., J. Phys. G 32 (2006) 151;
Q. Li, et al., J. Phys. G 32 (2006) 407.
[26] Th. Blaich, et al., Nucl. Instrum. Methods Phys. Res. A 314 (1992) 136.
[27] A. Gobbi, et al., Nucl. Instrum. Methods Phys. Res. A 324 (1993) 156.
[28] W. Reisdorf, et al., Nucl. Phys. A 612 (1997) 493.
[29] S.A. Bass, et al., Progr. Part. Nucl. Phys. 41 (1998) 225.
[30] Q. Li, M. Bleicher, J. Phys. G 36 (2009) 015111.
[31] Yingxun Zhang, Zhuxia Li, Phys. Rev. C 74 (2006) 014602.
[32] A. Andronic, J. Łukasik, W. Reisdorf, W. Trautmann, Eur. Phys. J. A 30 (2008) 31.
[33] A. Andronic, et al., Phys. Lett. B 612 (2005) 173.
[34] V. Giordano, et al., Phys. Rev. C 81 (2010) 044611.
[35] Qingfeng Li, Caiwan Shen, M. Di Toro, Mod. Phys. Lett. A 9 (2010) 669.
[36] W. Trautmann, et al., Prog. Part. Nucl. Phys. 62 (2009) 425;
W. Trautmann, et al., Int. J. Mod. Phys. E 19 (2010) 1653.